ELectronics EXpress

IEICE Electronics Express, Vol.8, No.8, 596–603

Novel III-V/Si hybrid laser structures with current injection across conductive wafer-bonded heterointerfaces: A proposal and analysis

Katsuaki Tanabe[a)], **Satoshi Iwamoto, and Yasuhiko Arakawa**

Institute for Nano Quantum Information Electronics and Institute of Industrial Science, University of Tokyo

4–6–1 Komaba, Meguro-ku, Tokyo 153–8505, Japan

a) *tanabe@iis.u-tokyo.ac.jp*

Abstract: We propose two novel III-V/Si hybrid laser structures with patterned window arrays in metal thin film wafer-bonding layers. The metal-mediated bonded III-V/Si heterointerface exhibits high electrical and thermal conductivity while allowing optical coupling between the III-V gain layer and the underneath Si waveguide through the openings in the metal bonding layer. We numerically examine the validity of the proposed hybrid laser structures through calculations of their modal propagation loss by metal's absorption and threshold current densities. We also propose another hybrid laser structure utilizing conductive direct semiconductor/semiconductor wafer bonding exploiting a spatial gain profile well overlapped with the waveguide mode and no metal-induced loss relative to those metal-mediated-bonded. All of these three structures have advantages such as spontaneous lateral current confinement and simpler fabrication over conventional oxide-mediated-bonded hybrid lasers.

Keywords: semiconductor lasers, metals, wafer bonding, silicon photonics

Classification: Optoelectronics, Lasers and quantum electronics, Ultrafast optics, Silicon photonics, Planar lightwave circuits

References

[1] A. W. Fang, H. Park, O. Cohen, R. Jones, M. J. Paniccia, and J. E. Bowers, "Electrically pumped hybrid AlGaInAs-silicon evanescent laser," *Opt. Express*, vol. 14, no. 20, pp. 9203–9210, Oct. 2006.

[2] J. Van Campenhout, P. Rojo-Romeo, P. Regreny, C. Seassal, D. Van Thourhout, S. Verstuyft, L. Di Cioccio, J.-M. Fedeli, C. Lagahe, and R. Baets, "Electrically pumped InP-based microdisk lasers integrated with a nanophotonic silicon-on-insulator waveguide circuit," *Opt. Express*, vol. 15, no. 11, pp. 6744–6749, May 2007.

DOI: 10.1587/elex.8.596
Received March 14, 2011
Accepted March 28, 2011
Published April 25, 2011

[3] K. Tanabe, M. Nomura, D. Guimard, S. Iwamoto, and Y. Arakawa, "Room temperature continuous wave operation of InAs/GaAs quantum dot photonic crystal nanocavity lasers on silicon substrate," *Opt. Express*, vol. 17, no. 9, pp. 7036–7042, April 2009.
[4] K. Tanabe, D. Guimard, D. Bordel, S. Iwamoto, and Y. Arakawa, "Electrically pumped 1.3 μm room-temperature InAs/GaAs quantum dot lasers on Si substrates by metal-mediated wafer bonding and layer transfer," *Opt. Express*, vol. 18, no. 10, pp. 10604–10608, May 2010.
[5] COMSOL Multiphysics ver. 4.0.
[6] P. B. Johnson and R. W. Christy, "Optical constants of the noble metals," *Phys. Rev. B*, vol. 6, no. 12, pp. 4370–4379, Dec. 1972.
[7] L. A. Coldren and S. W. Corzine, *Diode Lasers and Photonic Integrated Circuits*, Wiley, New Jersey, 1995.
[8] W. Spitzer and H. Y. Fan, "Infrared absorption in n-type silicon," *Phys. Rev.*, vol. 108, no. 2, pp. 268–271, Oct. 1957.
[9] D. K. Schroder, R. N. Thomas, and J. C. Swartz, "Free carrier absorption in silicon," *IEEE Trans. Electron Devices*, vol. 25, no. 2, pp. 254–261, Feb. 1978.
[10] RSOFT FullWAVE ver. 6.1.
[11] K. Tanabe, A. Fontcuberta i Morral, H. A. Atwater, D. J. Aiken, and M. W. Wanlass, "Direct-bonded GaAs/InGaAs tandem solar cell," *Appl. Phys. Lett.*, vol. 89, no. 10, pp. 102106-1–102106-3, Sept. 2006.
[12] K. Tanabe, D. Guimard, and Y. Arakawa, unpublished.

1 Introduction

III-V/Si hybrid lasers [1, 2] are promising for realization of photonic integrated circuits. In 2009 and 2010, we have experimentally demonstrated InAs/GaAs quantum dot lasers on Si substrates fabricated by SiO_2- and metal-mediated GaAs/Si wafer bonding, respectively, and suggested that patterned arrays of windows in those SiO_2 or metal bonding layers would enable evanescent optical coupling between the III-V gain and underneath Si waveguides to realize hybrid lasers [3, 4]. In this present work, we propose two novel III-V/Si hybrid laser structures with metal bonding layers. In contrast to oxide-mediated bonding used for hybrid laser fabrication to date [1, 2], metal-mediated bonding provides higher electrical and thermal conductivity to wafer-bonded III-V/Si heterointerfaces and also can increase roughness tolerance for bonding surfaces while lowering required bonding temperature. Highly conductive metal-mediated-bonded heterointerfaces also enable vertical carrier injection, which prevents current spreading toward laser stripe edges. Therefore, our structures have advantages of higher quantum efficiencies and simpler fabrication without mesa etch or ion implantation for carrier confinement required in fabrication of the previous lateral-current-injection III-V/Si hybrid lasers. We numerically examine the validity of the proposed hybrid laser structures through calculations of their modal propagation loss by metal's absorption and threshold current densities. We also propose another hybrid laser structure utilizing conductive direct semiconductor/semiconductor wafer bonding, which has advantages over those metal-

DOI: 10.1587/elex.8.596
Received March 14, 2011
Accepted March 28, 2011
Published April 25, 2011

IEICE Electronics Express, Vol.8, No.8, 596–603

mediated-bonded of simpler fabrication as well as higher efficiency by better overlap of spatial gain profile with the waveguide mode.

2 III-V/Si hybrid lasers with bonding metal stripes I: *Ski* structure

2.1 Overview of the structure

Firstly, we propose a III-V/Si hybrid laser structure, schematically shown in Fig. 1 (a), with two metal strips positioned along and on both side edges of a Si rib waveguide like a pair of ski boards (named *Ski* structure), to maximize optical coupling between the III-V gain layer and the Si waveguide and to minimize absorption loss by metal, because the fundamental optical mode has its maximum intensity at the center of the Si waveguide in lateral direction.

2.2 Optical confinement factors and modal propagation loss

We calculated the optical confinement factors in the III-V multi quantum wells (MQWs), Γ_{MQW}, and the Si rib waveguide, Γ_{Si}, and modal propagation loss induced by metal's absorption, α_i^{metal}, in the proposed hybrid laser structure by two-dimensional finite element method (FEM) [5]. We adopted the materials and dimensions of the 1.55 μm AlInGaAs MQW/Si hybrid laser with a 2 μm-wide Si rib waveguide in Ref. 1 except for our bonding metal components. The complex refractive index of silver in Ref. 6 was used for the bonding metal strips and α_i^{metal} was calculated from the imaginary part of the propagation constants. Γ_{MQW} and Γ_{Si} were calculated by two-dimensional integration of power density.

Fig. 1 (b) shows the calculated dependence of Γ_{MQW}, Γ_{Si} and α_i^{metal} on the width of each metal strip, w, for the metal bonding layer thickness, h, of 100 nm. There are local maxima of α_i^{metal}, as seen in Fig. 1 (b), by field concentration at the metal surface due to surface plasmon resonance. Some specific values of w strongly supports localized surface plasmon modes of lower to higher order corresponding to smaller to larger w, as we observed for h = 10 nm the number of the field nodes of 2, 3 and 4 in each metal strip for w = 120, 320 and 520 nm. α_i^{metal} however can be suppressed to below 10 cm^{-1} by proper choice of w to avoid plasmon resonance, as seen in Fig. 1 (b).

2.3 Threshold current densities

From Γ_{MQW} and α_i^{metal} calculated in the previous section, we estimated the lasing threshold current densities, J_{th}, using a conventional coupled rate model [7] resulting in:

$$J_{th} \cong \frac{qH}{\eta_i} B N_{tr}^2 \exp\left(2\frac{\alpha_i + \alpha_m}{\Gamma_{MQW} g_0}\right), \quad (1)$$

where H is the total MQW thickness assumed to be 56 nm (7 nm × 8 wells) as in Ref. 1, η_i is the internal quantum efficiency assumed to be 0.5, B is the

DOI: 10.1587/elex.8.596
Received March 14, 2011
Accepted March 28, 2011
Published April 25, 2011

EL ectronics
EX press

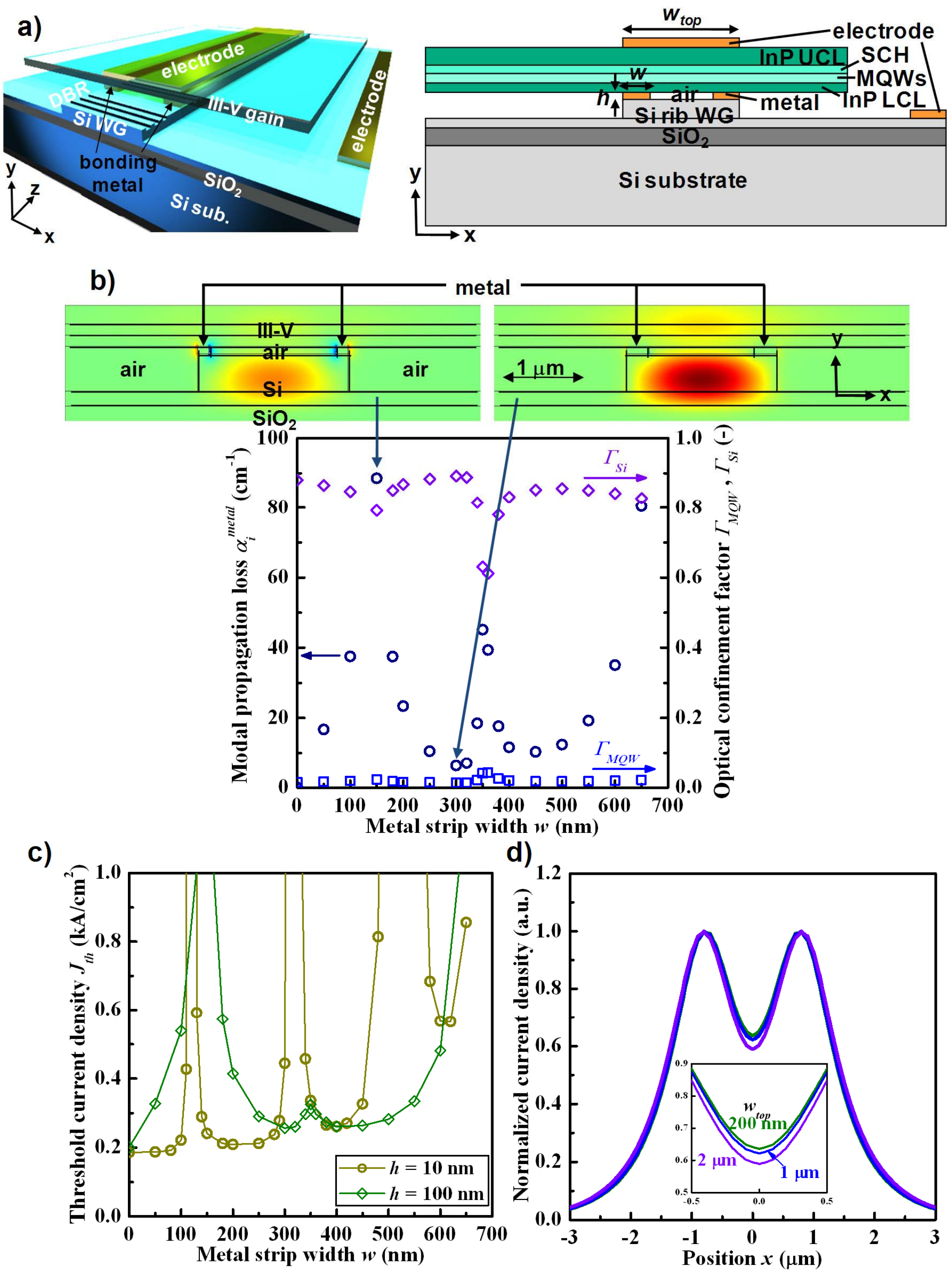

Fig. 1. *Ski* structure hybrid laser: (a) schematic, (b) mode profiles (E_x), Γ_{MQW}, Γ_{Si} and α_i^{metal} for $h =$ 100 nm, (c) J_{th} and (d) current density profiles at the MQWs for $h = 100$ nm, $w = 300$ nm. In this structure, distributed Bragg reflector (DBR) or distributed feedback (DFB) structures are implemented either in the Si rib waveguide or the III-V gain layer to form a laser cavity while enabling coupling into Si photonic circuits.

bimolecular recombination coefficient, 10^{-10} cm^3/s as in Ref. 7 and N_{tr} is the transparency carrier density, 1×10^{18} cm^{-3} as in Ref. 7. α_i is the modal propagation loss, typically around 2 cm^{-1} for conventional semiconductor lasers and much smaller than α_i^{metal} we calculate. In this paper, we therefore input α_i^{metal} for this α_i, neglecting non-metallic loss such as free carrier absorption

DOI: 10.1587/elex.8.596
Received March 14, 2011
Accepted March 28, 2011
Published April 25, 2011

IEICE Electronics Express, Vol.8, No.8, 596–603

and roughness-induced scattering. α_m is the mirror loss calculated for the laser cavity length of 300 μm and facets reflectivity of 0.9/0.9 assuming DBR or DFB. g_0 is the coefficient in an empirical gain formula $g = g_0 \ln(N/N_{tr})$, 4000 cm^{-1} as in Ref. 7.

Note that J_{th}'s of waveguide-coupled hybrid lasers are unavoidably larger than those of conventional semiconductor lasers because of the significantly smaller Γ_{MQW} due to the shared optical mode mainly lying in the Si part. Fig. 1 (c) shows the calculated J_{th} of our proposed hybrid lasers with varied h and w. J_{th} for $h = 100$ nm and $w = 300$ nm for example was estimated to be 300 A/cm^2 with $\Gamma_{MQW} = 0.014$, relative to 2 kA/cm^2 with $\Gamma_{MQW} = 0.03$ reported in Ref. 1, and suitable for practical use.

2.4 Lateral current confinement

One of the advantages of our proposed structure is current confinement in lateral direction by carrier injection across the wafer-bonded heterointerfaces and through the Si rib. To verify this merit, we calculated the current density profile in our hybrid laser structure by two-dimensional FEM [5]. We used 1 Ω cm for the resistivity of the III-V and Si region, corresponding to doping concentration of around 10^{16} cm^{-3}, and 1×10^{-4} Ω cm^2 for the metal/semiconductor interfacial contact resistance, although their variation hardly affect the current density profile result as we tested. Note that for this doping concentration additive α_i induced by free carrier absorption is on the order of 0.1 cm^{-1} at 1.55 μm [8, 9], much smaller than α_i^{metal} calculated in Section 2.2, and therefore negligible.

Fig. 1 (d) shows the current density profiles in the lateral direction at the MQW region for $h = 100$ nm, $w = 300$ nm and varied width of the top metal electrode, w_{top}. It is seen for all w_{top}'s that the current flow is laterally confined in the III-V gain region above the Si rib waveguide and nicely overlap with the optical mode shown in the inset of Fig. 1 (b). In this way, injected carriers are efficiently used in the III-V MQW gain region to couple to the lasing mode to realize high η_i in our structure even without mesa etch or ion implantation conducted for hybrid laser fabrication to date. In addition, it is interestingly found that narrowing w_{top} gives a small increase of uniformity in current density profile as seen in Fig. 1 (d) by mitigating the current localization above the two metal strips by the intermediate positioning of the top electrode.

3 III-V/Si hybrid lasers with bonding metal stripes II: *Ladder* structure

3.1 Overview of the structure

Secondly, we propose another III-V/Si hybrid laser structure with bonding metal stripe orthogonal to the Si rib waveguide like ladder steps (named *Ladder* structure), schematically depicted in Fig. 2 (a). This structure may have more optical absorption loss by metal than the *Ski* structure proposed in Section 2 because the metal stripe lies throughout the width of the Si rib,

DOI: 10.1587/elex.8.596
Received March 14, 2011
Accepted March 28, 2011
Published April 25, 2011

ELectronics EXpress

not only on the rib edges as in *Ski* structure. However, its fabrication process may be simpler than that of *Ski* structure with no need of precise alignment of the metal stripe to the Si rib.

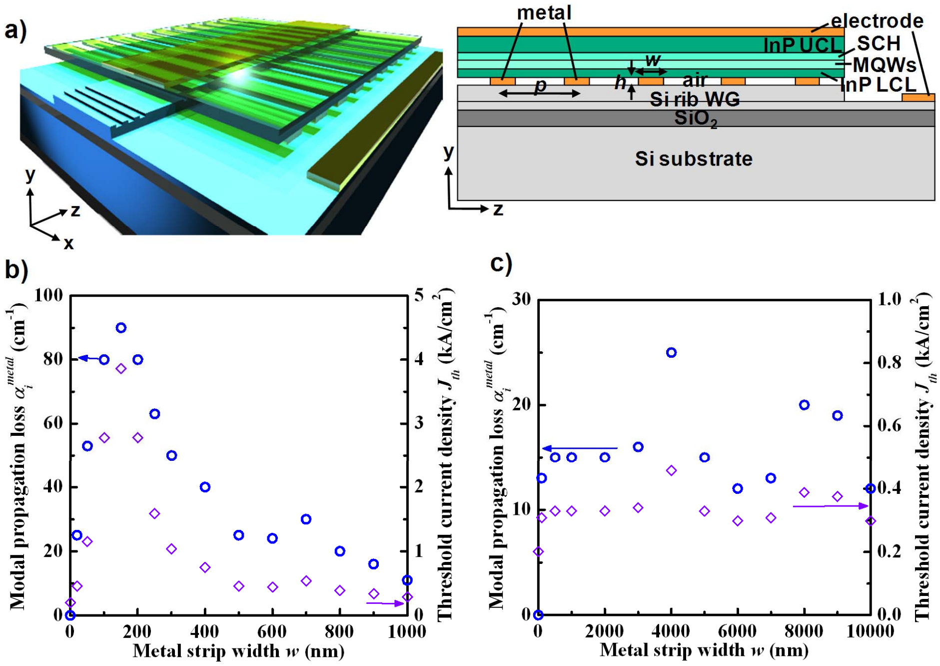

Fig. 2. *Ladder* structure hybrid laser: (a) schematic, α_i^{metal} and J_{th} for $p =$ (b) 1 μm and (c) 10 μm.

3.2 Modal propagation loss and threshold current densities

We calculated α_i^{metal} of this *Ladder* hybrid laser structure by three-dimensional finite difference time domain method [10]. Same materials and dimensional parameters to those adopted in Section 2 were used for this calculation, except for the metal strip width w defined to the direction parallel to the Si rib waveguide. We also estimated J_{th} similarly in Section 2 from the calculated α_i^{metal} and Γ_{MQW} assumed to be 0.015, equal to that of the structure without metal stripe, i.e. $w = 0$. These results with varied w for $h = 100\,$nm and metal stripe pitches p of 1 and 10 μm are summarized in Fig. 2 (b) and (c), respectively. Even by this weak optimization, we find structural conditions for modest α_i^{metal} around 10 cm^{-1} and J_{th} around 300 A/cm^2 and further dimensional optimization would give us higher performance. Although α_i^{metal} is found small around at 100% metal coverage regions, i.e. $w \sim p$, we should rather adopt other local minima at 50 - 60% coverage to ensure optical coupling. Additionally, we have to care for particularly large p ($> 1\,\mu$m) cases for spatial current nonuniformity, dissimilar to smaller p cases represented by Fig. 1 (d), which may lead to larger J_{th} than in Fig. 2 (c) calculated under the assumption of uniform current profiles.

DOI: 10.1587/elex.8.596
Received March 14, 2011
Accepted March 28, 2011
Published April 25, 2011

4 III-V/Si hybrid lasers by direct wafer bonding

4.1 Overview of the structure

Thirdly, we propose III-V/Si hybrid lasers by using direct semiconductor/semiconductor wafer bonding, as schematically depicted in Fig. 3 (a). In this absence of metal component, there is no concern for absorption loss in the laser cavities. Although direct bonding is generally considered more difficult than oxide- and metal-mediated bonding, we have recently succeeded in GaAs/InP [11] and GaAs/Si [12] direct bonding to obtain highly conductive Ohmic heterojunctions.

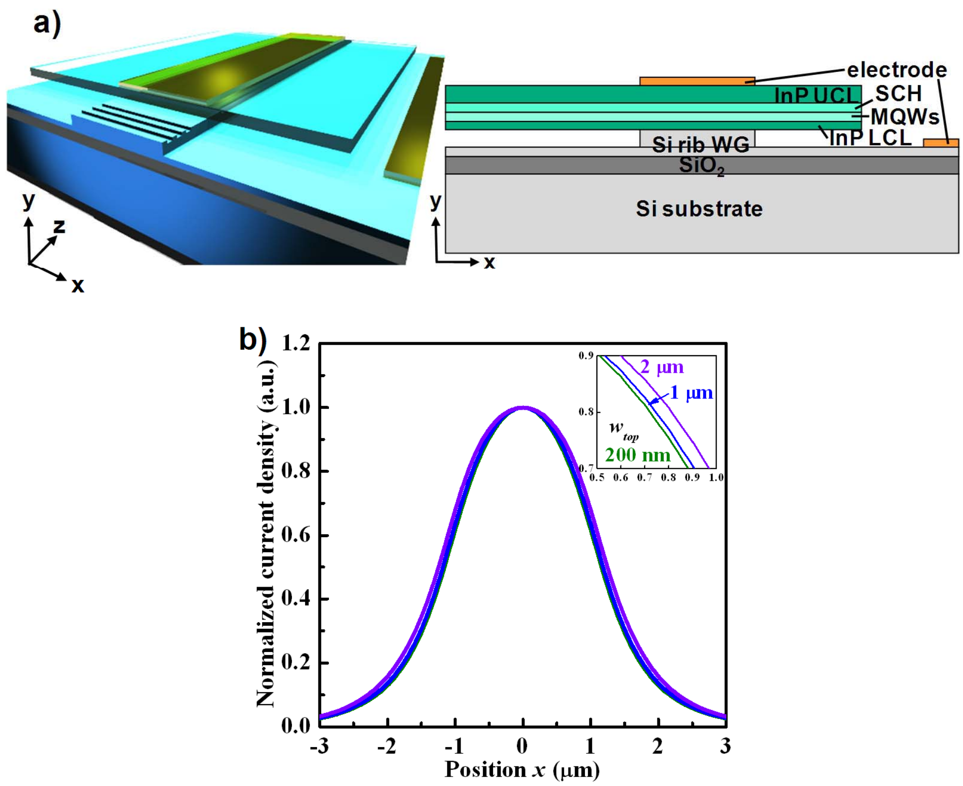

Fig. 3. Direct-bonded hybrid laser: (a) schematic and (b) current density profiles at the MQWs.

4.2 Threshold current density

We calculated Γ_{MQW} and Γ_{Si} for this direct-bonded hybrid laser structure by two-dimensional FEM in a similar manner as in Section 2.2 to be 0.048 and 0.65, respectively. We then calculated J_{th} using this Γ_{MQW} and α_i assumed to be $2\,\mathrm{cm}^{-1}$ similarly in Section 2.3. The resulted J_{th} was $200\,\mathrm{A/cm}^2$, mostly smaller than J_{th} for the metal-mediated-bonded structures calculated in Sections 2.3 and 3.2 thanks to the smaller α_i in the metal-free waveguide.

4.3 Lateral current confinement

Excellent lateral current confinement is observed as shown in Fig. 3 (b) in the similar current density profile calculations as in Section 2.4 except for

DOI: 10.1587/elex.8.596
Received March 14, 2011
Accepted March 28, 2011
Published April 25, 2011

ELectronics EXpress
IEICE Electronics Express, Vol.8, No.8, 596–603

$1 \times 10^{-1}\,\Omega\ cm^2$ used for the interfacial resistance at the III-V/Si direct-bonded interface reflecting our experimental results. In contrast to the dual-peaked current density profiles for *Ski* structure shown in Fig. 1 (d), the current profiles for this direct-bonded structure in Fig. 3 (b) fit the optical mode in the inset of Fig. 1 (b) well with single maxima at the center in the lateral direction. The direct-bonded hybrid laser structure this way would have a significant advantage of more efficient excitation of the fundamental waveguide mode thanks to the spatial distribution of gain well overlapped with the mode over the metal-mediated-bonded structures.

5 Conclusion

In this work, we have proposed three types of III-V/Si hybrid laser structures utilizing conductive wafer-bonded III-V/Si heterointerfaces. Our structures enable vertical current injection across the bonded heterinterfaces and therefore have advantages of lateral current confinement leading to higher quantum efficiencies and simpler fabrication without mesa etch or ion implantation in contrast to the previous lateral-current-injection III-V/Si hybrid lasers using SiO_2-mediated wafer bonding. While metal-mediated bonding eases bond and enhances thermal and electrical conductivities, direct bonding would ideally provide simpler fabrication and higher efficiency by lower absorption loss and better gain-mode overlap.

Acknowledgments

This research was supported by JSPS through FIRST Program, MEXT Japan through the Special Coordination Funds for Promoting Science and Technology and Kakenhi 21860017, and Intel Corporation.

DOI: 10.1587/elex.8.596
Received March 14, 2011
Accepted March 28, 2011
Published April 25, 2011